processing speed? We propose an output-scheduling control employing a pipelining technique, which has been extensively used for parallel processing systems.

An example of the first implementation of the proposed control is shown in Fig. 2*b*. It allows an input controller to send several requests, for cell x and cell y in Fig. 2*b*, to the contention controller consecutively. The contention controller accepts and processes them in a batch mode and returns the assigned times. Consequently, all the processing sequences for the two cells are completed within two cell slots, assuring no decrease in throughput. Thus, the first implementation reduces the equivalent propagation delay time to t_d/n (n the number of processed cells in a batch). Note that cells incur a fixed delay time of n cells. The output-scheduling control is executed independently for each output port and the reservation of the sending table is made in a first-come, first-served mode. There is no interference between cell x and cell y when their destination addresses are different from each other. However, if their destination addresses are the same and cell x fails to make a reservation at the assigned slot t_x while cell y makes a successful reservation at the assigned slot t_y, then cell x and cell y must change the assigned times; cell x instead of y will be sent at t_y. Cell y retries the contention control along with the next cell in the input buffer because cell y is assigned to t_x, where the sending table has already been reserved by another cell. This exchange of the assigned times is necessary to maintain the cell sequence on a virtual path or circuit provided through ATM switches.

An example of the second implementation of the pipelined output-scheduling control is shown in Fig. 2*c*. The request signal of cell y is sent from the input to the contention controller before the input receives the assigned time for cell x. The scheduling processes for cell x and cell y are overlapped but no identical processes run simultaneously, i.e. the scheduling control runs in a pipeline mode. This assures easy design of contention control circuits for this second type of implementation. The TAT exceeds one cell slot but an input controller sends a request of a cell and receives its assigned slot during each cell slot as shown in Fig. 2*c*. These features due to pipelining prevent a decrease in the throughput of the switch. The exchange of the assigned times as described in the first implementation is also necessary in the second implementation for the same reason.

There is a tradeoff between hardware complexity and incurred delay time in the first and second implementations. There is less hardware complexity and larger delay time in the first implementation and vice versa in the second. Although this Letter focuses on an output-scheduling algorithm, the proposed parallel control with a slight modification can be applied to a three-phase algorithm. It seems rather complex to apply the proposed control to a window-selection algorithm because several cells awaiting in an input buffer are processed during a cell slot.

Suppose, for example, that the distance between an input controller and a centralised contention controller is 100 feet and input and output port speed is 2·4 Gbit/s. The length of the cell time slot is about 170 ns and $n = 4$ is sufficient for the first implementation. If the contention controller circuit described in Reference 2 is employed and a 400×400 switch size is assumed, the contention control circuit operates at ~ 150 MHz clock rate and has 16 bus lines, each of which is 9 bits wide. These observations suggest the possibility of designing a contention controller for an input queueing ATM switch of 1 Tbit/s capacity. Such a high capacity fabric may be developed by BSB switch architecture [6], which we believe to be one of the most promising candidates for high capacity ATM switches.

Conclusion: Parallel contention control for input queueing ATM switches has been proposed to overcome the propagation delay time between an input controller and a centralised contention controller. Although this Letter has described a design of the parallel control for an output-scheduling algorithm, the proposed control may be effective for other contention resolution algorithms. By employing the proposed parallel control to an output-scheduling algorithm, a potential design of a contention controller for ATM switches with an aggregate capacity of 1 Tbit/s is suggested.

Acknowledgment: The authors would like to thank I. Tokizawa, T. Aoyama, and T. Miki of NTT Transmission Systems Laboratories for supporting this work. They also wish to thank B. Jabbari at George Mason University for helpful comments on this subject, presented by one of the authors at ICC '90.

4th March 1992

H. Obara and Y. Hamazumi (*NTT Transmission Systems Laboratories, Room 807C, NTT, 1-2356 Take, Yokosuka, 238 Japan*)

References

1 OBARA, H., and YASUSHI, T.: 'High speed transport processor for broadband burst transport system'. Proc. IEEE Int. Conf. on Communications, Philadelphia, 1988, pp. 922–927

2 OBARA, H., SASAGAWA, M., and TOKIZAWA, I.: 'An ATM cross-connect system for broadband transport networks based on virtual path concept'. Proc. of the IEEE Int. Conf. on Communications, Atlanta, 1990, pp. 839–843

3 HUI, J. Y., and ARTHURS, E.: 'A broadband packet switch for integrated transport', *IEEE J. Sel. Areas Commun.*, 1987, **SAC-5**, (8), pp. 1264–1273

4 UEMATSU, H., MATSUNAGA, H., and OBARA, H.: 'A cell based cross-connect switch for ATM broadband networks'. Proc. of Singapore Int. Conf. on Networks, Singapore, 1989, pp. 371–376

5 OBARA, H.: 'Optimum architecture for input queueing ATM switches', *Electron. Lett.*, 1991, **27**, (7), pp. 555–556

6 OBARA, H., OKAMOTO, S., and HAMAZUMI, Y.: 'Input and output queueing ATM switch architecture with spatial and temporal slot reservation control', *Electron. Lett.*, 1992, **28**, (1), pp. 22–24

PERFORMANCE ANALYSIS OF MICROCELLULAR MOBILE RADIO SYSTEMS WITH SHADOWED COCHANNEL INTERFERERS

Y.-D. Yao and A. U. H. Sheikh

Indexing terms: Mobile radio systems, Interference

A study is presented of microcellular mobile radio systems where the desired signal has Rician statistics and cochannel interferers experience lognormal shadowing as well as Rayleigh fading. This implies a Rician/Rayleigh-plus-lognormal microcell interference model. The probability density function of the signal-to-interference ratio is derived and used to evaluate the performance of microcellular systems in terms of the outage probability.

Introduction: Extensive studies on the effects of cochannel interference in medium/large cell systems have been conducted [1–3]. Models from Rayleigh fading [1], lognormal shadowing [2] to superimposed Rayleigh fading and lognormal shadowing [5] hve been used to characterise signal propagation environments. There is a common assumption in all these studies, however, that all signals received, desired and undesired, have the same statistical characteristics. For example, in Reference 1, the desired signal as well as undesired cochannel interferers are assumed to be subject to Rayleigh fading. To evaluate the performance of microcellular mobile radio systems, a microcell interference model, in which different fading statistics are used to characterise the desired and undesired signals, is introduced in Reference 4. The desired signal is assumed to have Rician statistics implying that a dominant multipath reflection exists in within-cell transmission [5]. The interference signals from cochannel cells are assumed to be subject to Rayleigh fading because of the absence of a line-of-sight propagation. This is the Rician/Rayleigh microcell interference model [4]. This model has been used to study the outage probability, bit error probability and spectral efficiency of microcellular mobile radio systems [4–7].

In a practical mobile radio system, the interferers are usually shadowed by surrounding obstructions such as buildings [2, 3]. Based on the Rician/Rayleigh model, this Letter further investigates the microcell interference issue by considering that the cochannel interferers are subject to lognormal shadowing as well as Rayleigh fading (superimposed Rayleigh fading and lognormal shadowing). This results in a Rician/Rayleigh-plus-lognormal interference model. Note that, in this model, we assume that the desired signal is transmitted through a line-of-sight propagation path within a microcell without experiencing shadowing. The probability density function (PDF) of the power ratio between the desired and interfering signals is first derived and then used to evaluate the performance of microcellular mobile radio systems in terms of the outage probability.

Rician/Rayleigh-plus-lognormal microcell interference model: In the Rician/Rayleigh-plus-lognormal microcell interference model, the envelope of the desired signal has Rician statistics. The PDF of the corresponding signal power, x, is

$$p_x(x) = \frac{1}{X}\exp\left(-\frac{2x+s^2}{2X}\right)I_0\left(\frac{\sqrt{(2x)}s}{X}\right) \tag{1}$$

where $I_0(\,)$ is the modified Bessel function of the first kind and order zero. The mean signal power is $X + s^2/2$, where X is contributed by the diffused signal component and $s^2/2$ by the direct line-of-sight signal component.

The cochannel interferers are subject to superimposed Rayleigh fading and lognormal shadowing; i.e. each interferer is a Rayleigh phasor [8] with a slowly varying local mean power. The local mean power is a random variable with lognormal statistics and the mean of the random variable is called the area mean power of the interferer. The total interference in the system is a sum of all interferers and the addition can be coherent or noncoherent. If the fading process is slow, the addition is considered to be coherent [9] and all cochannel interferers (Rayleigh phasors) add up to one Rayleigh phasor [8, 9]. The mean power of the composite Rayleigh phasor is a sum of the lognormally distributed local mean powers of all interferers. Following References 10 and 11, the sum of lognormal random variables is well approximated by another lognormal random variable. Thus, the total interference is characterised by superimposed Rayleigh and lognormal statistics. Denoting the total interference power as y, we have a conditional PDF [3, 8]

$$p_{y|Y}(y\,|\,Y) = \frac{1}{Y}\exp\left(-\frac{y}{Y}\right) \tag{2}$$

where Y is the local mean power of the composite interference with a PDF [3, 8]

$$p_Y(Y) = \frac{C}{Y}\exp\left[-\frac{(\log Y + A)^2}{B}\right] \tag{3}$$

In eqn. 3, $C = (\log e)/[\sqrt{(2\pi)}\sigma]$, $A = -\log Y_0 + \sigma^2/(2\log e)$, and $B = 2\sigma^2$. Y_0 is the area mean power of the composite interference and σ is the standard deviation in bels.

Defining the signal-to-interference power ratio as $r = x/y$, we derive the PDF of r as follows:

$$P_R R- = \int_0^\infty y p_x(ry) \int_0^\infty p_{y|Y}(y\,|\,Y)p_Y(Y)\,dY \quad dy$$

$$= C\int_0^\infty \frac{(a+1)rZ+1}{(rZ+1)^3} \times \exp\left\{-\frac{1}{B}\left[\log(bZ) + \frac{B}{4}\ln 10\right]^2 - \frac{a}{rZ+1}\right\} dZ \tag{4}$$

where $a = s^2/(2X)$ and $b = X/Y_0$.

In the following, we use the PDF $p_r(r)$ to derive the outage probability of microcellular systems.

Performance analysis: In a slow fading environment, the outage probability is an appropriate measure to evaluate the performance of a mobile radio system. The outage probability is defined as the probability of failing to achieve simultaneously a signal-to-noise ratio (SNR) and a signal-to-interference ratio (SIR) sufficient to give satisfactory reception [1 4]. A simpler analysis may consider only one of the two requirements, either SNR or SIR, for system evaluation. For example, in an interference-limited environment, we need consider only the SIR requirement. Assuming that the signal-to-interference protection ratio is R_I, the outage probability is derived as

$$P_{out} = \text{prob}\,\{r < R_I\} = \int_0^{R_I} p_r(r)\,dr = CR_I\int_0^\infty \frac{1}{R_I Z + 1} \times \exp\left\{-\frac{1}{B}\left[\log(bZ) + \frac{B}{4}\ln 10\right]^2 - \frac{a}{R_I Z+1}\right\} dZ \tag{5}$$

If both the SNR requirement (assuming that the minimum required desired signal power is $R_N X$) and the SIR requirement are considered, the outage probability is found to be

$$P_{out} = 1 - \text{prob}\,\{x > R_N X,\ x/y > R_I\} = 1 - \int_{R_N X}^\infty \left[\int_0^{x/R_I} p_y(y)\,dy\right] p_x(x)\,dx$$

$$= 1 - Q[\sqrt{(2a)}, \sqrt{(2R_N)}] + CR_I\int_0^\infty \frac{1}{R_I Z+1} \times \exp\left\{-\frac{1}{B}\left[\log(bZ) + \frac{B}{4}\ln 10\right]^2 - \frac{a}{R_I Z+1}\right\} \times Q\left\{\sqrt{\left(\frac{2aR_I Z}{R_I Z+1}\right)}, \sqrt{\left[2\left(1+\frac{1}{R_I Z}\right)R_N\right]}\right\} dZ \tag{6}$$

where $Q(\,,\,)$ is the Q function.

The outage probability given in eqns. 5 or 6 is usually used to assess the performance of mobile radio systems under very slow fading conditions. If the channel fading is slow compared to the data rate but fast compared to the message duration, the bit error probability is used to measure the system performance. Note that, under such fading rate conditions, the assumption of coherent addition of interferers is still valid at least on a bit-by-bit basis. Therefore, the PDF given in eqn. 4 can be used to derive the bit error probability.

There are classical results for the optimum detection of nonfading binary signals when the channel is perturbed by Gaussian noise. For example, the 'static' probability of bit error (in a nonfading environment) is expressed in an exponential function of signal-to-noise ratio for noncoherent frequency shift keying or differential phase shift keying signals. When the channel is subject to fading, the signal-to-noise ratio is a random variable and the 'dynamic' bit error probability is derived by averaging the 'static' probability over all possible values of the signal-to-noise ratio. This method can also be used to derive the bit error probability when the signal is subject to interfering in a fading environment [7, 12]. Following this approach, the bit error probability in a microcellular system with faded and shadowed interferers is easily obtained.

Numerical results and conclusions: Assuming $a = 5$ and $R_I = 5$, the numerical results of eqn. 5 are presented in Fig. 1. Three cases with $\sigma = 6$, 10 and 12 dB, respectively, are shown. The case without shadowing is also shown in the Figure for comparison. It is observed that the presence of shadowing in the interfering signal transmission path affects the performance of microcellular systems significantly. It is interesting to find that, under low signal-to-interference ratio ($b = X/Y_0$, i.e. the ratio between the mean power of the signal and the area mean power of the interference) conditions, a lower outage probability is achieved when the interferers experience heavier shadowing. Under high signal-to-interference ratio conditions, however, the outage probability increases due to heavier shadowing.

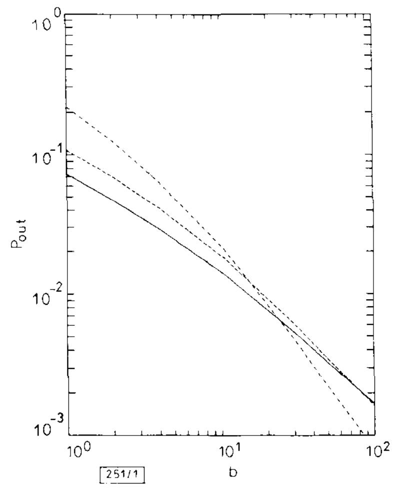

Fig. 1 *Shadowing effect on outage probability*

······ no shadowing
—·—· $\sigma = 10$ dB
——— $\sigma = 12$ dB

In conclusion, this Letter presents a Rician/Rayleigh-plus-lognormal microcell interference model. The PDF of the signal-to-interference ratio is derived and used to evaluate the microcellular system performance. It is observed that, owing to the shadowing effect on the cochannel interferers, the system outage probability is reduced or increased depending on the operating X/Y_0 range.

2nd March 1992

Y.-D. Yao (*Communications Group, Spar Aerospace Limited, Ste-Anne-de-Bellevue, Quebec H9X 3R2, Canada*)

A. U. H. Sheikh (*Dept. of Systems and Computer Eng., Carleton University, Ottawa, Ontario K1S 5B6, Canada*)

References

1 SOWERBY, K. W., and WILLIAMSON, A. G.: 'Outage probability calculations for a mobile radio system having multiple Rayleigh interferers', *Electron. Lett.*, 1987, **23**, pp. 600–601

2 YEH, Y. S., and SCHWARTZ, S. C.: 'Outage probability in mobile telephony due to multiple log-normal interferers', *IEEE Trans.*, 1984, **COM-32**, pp. 380–387

3 WILLIAMSON, A. G., and PARSONS, J. D.: 'Outage probability in a mobile radio system subject to fading and shadowing', *Electron. Lett.*, 1985, **21**, pp. 622–623

4 YAO, Y. D., and SHEIKH, A. U. H.: 'Outage probability analysis for microcell mobile radio systems with cochannel interferers in Rician/Rayleigh fading environment', *Electron. Lett.*, 1990, **26**, pp. 864–866

5 BULTITUDE, R. J. C., and BEDAL, G. K.: 'Propagation characteristics on microcellular urban mobile radio channels at 910 MHz', *IEEE J. Sel. Areas Commun.*, 1989, **SAC-7**, pp. 31–39

6 PRASAD, R., KIEGEL, A., and OLSTHOORN, J.: 'Spectrum efficiency analysis for microcellular mobile radio systems', *Electron. Lett.*, 1991, **27**, pp. 423–425

7 YAO, Y. D., and SHEIKH, A. U. H.: 'Bit error probabilities of NCFSK and DPSK signals in microcellular mobile radio systems', *Electron. Lett.*, 1992, **28**, pp. 363–364

8 PRASAD, R., and ARNBAK, J. C.: 'Enhanced packet throughput in radio channels with fading and shadowing'. Proc. Canadian Conf. Electrical and Computer Eng., 1988, pp. 78–80

9 ARNBAK, J. C., and BLITTERSWIJK, W.: 'Capacity of slotted ALOHA in Rayleigh-fading channels', *IEEE J. Sel. Areas Commun.*, 1987, **SAC-5**, pp. 261–269

10 FENTON, L. F.: 'The sum of log-normal probability distributions in scatter transmission systems', *IRE Trans. Commun. Syst.*, 1960, **CS-8**, pp. 57–67

11 SCHWARTZ, S. C., and YEH, Y. S.: 'On the distribution function and moments of power sums with log-normal components', *Bell Syst. Tech. J.*, 1982, **61**, pp. 1441–1462

12 WOJNAR, A. H.: 'Unknown bounds on performance in Nakagami channels', *IEEE Trans.*, 1986, **COM-34**, pp. 22–44

DESIGN OF RIDGE WAVEGUIDE COUPLERS WITH CARRIER INJECTION USING DISCRETE SPECTRAL INDEX METHOD

S. V. Burke, M. J. Adams, P. C. Kendall, P. N. Robson and G. J. Rees

Indexing terms: Integrated optics, Waveguide couplers

It is shown that the design of ridge waveguide couplers with a uniformly layered refractive index profile can be extended to include the nonuniformity arising within an active layer as a result of carrier injection. This is analysed using the spectral index method combined with a degenerate perturbation approach. The simplicity of this approach makes it possible to solve design problems in which the correct mixing of the fields beneath the ridges is an essential feature of the modelling, and necessary for accuracy of design.

Ridge, rib and other two-dimensional waveguides are becoming increasingly important for applications in integrated optics. They confine the light both laterally and vertically and, with improvements in III-V semiconductor technology, a greater control over device dimensions and indices can now be achieved. Despite their simple structure, rib waveguides are difficult to model. Finite difference and finite element methods are undeniably accurate and versatile but require much processing power and are difficult to implement. Approximate methods such as the effective index (EI) method can only be applied with confidence to a limited range of problems [1]. The discrete spectral index (DSI) method in comparison has been established as both a fast and accurate technique for modelling single rib waveguides, and symmetric and asymmetric couplers [2]. To implement the DSI method, which is variational, the structure is divided into three regions: the cladding which is assumed to be air, the ribs, and the layered region below the ribs. The field is set to zero on the semiconductor/air interfaces using the method of false position. The polarised wave equation is then solved exactly but independently both in and below the ribs. In the ribs trigonometric or hyperbolic trial functions are selected by assuming that E, the relevant field component, is of the form $E = F(x)G(y)$ where x and y are perpendicular co-ordinates in the cross-section of the guide. Below the ribs the field is expressed as a Fourier series which has the effect of eliminating the lateral dependency of the problem and results in a solution which is similar to that of a planar slab. The two solutions are then linked across the bases of the ribs by the variational technique, equivalent to continuity of stored power. A dispersion equation has thus been constructed. For couplers, the propagation constants β_s and β_a for the lowest-order symmetric and antisymmetric supermodes are obtained. The DSI method also generates accurate field profiles. From β_s and β_a the coupling length, a critical parameter for device design, is obtained.

A necessary requirement of the DSI method is that the layers below the ribs (any number of which can be accommodated) must each be of uniform refractive index. However, many optoelectronic coupler devices rely on small nonuniform changes in index for their operation. For example, a twin-guide laser amplifier consisting of two coupled ridge waveguides experiences small index changes in the active layer as a consequence of carrier injection. By varying the current ratio between the guides, the structure can